

ACCOUNTING FOR NEAR-SOURCE EFFECTS IN THE DISPLACEMENT COEFFICIENT METHOD FOR SEISMIC STRUCTURAL ASSESSMENT

Georgios Baltzopoulos, Eugenio Chioccarelli and Iunio Iervolino

Dipartimento di Strutture per l'Ingegneria e l'Architettura, Università degli Studi di Napoli Federico II
Via Claudio 21, 80125, Naples, Italy.

e-mail: georgios.baltzopoulos@unina.it, eugenio.chioccarelli@unina.it, iunio.iervolino@unina.it

Keywords: directivity, performance-based seismic design.

Abstract. *Non-linear static procedures are well-established analytical tools for performance-based seismic design and assessment. On the other hand, near-source (NS) ground motions are emerging as relevant to structural engineering because they may be characterized by seismic demand larger and systematically different than that typically induced by so-called ordinary records. This is the result of phenomena such as rupture forward directivity (FD), which may lead to the appearance of distinct velocity pulses in the ground motion velocity time-history. Lately, effort was put towards the framework necessary for taking FD into account in probabilistic seismic hazard analysis (PSHA). The objective of the present study is to discuss the extension of non-linear static procedures, such as the displacement coefficient method (DCM), with respect to the inelastic demand associated with FD. In this context, the DCM is implemented to estimate NS seismic demand by making use of the results of NS-PSHA, developed for single-fault-case scenarios. A predictive model for NS-FD inelastic displacement ratios, previously developed by the authors, is employed. An illustrative application of the DCM, with explicit inclusion of NS-pulse-like effects, is given for a plane R/C frame designed under modern code provisions.*

1 INTRODUCTION

Sites located in the vicinity of seismic faults may experience ground motions which can be considered *atypical* due to phenomena collectively known as near-source (NS) effects. Most important among these effects, is forward rupture directivity (FD). During fault rupture, shear dislocation may propagate at velocities similar to the shear wave velocity; as a result, there is a probability that at sites aligned along the direction of rupture propagation, shear wave-fronts generated at different points along the fault arrive at the same time, delivering most of the seismic energy in a single double-sided pulse registered early in the velocity recording. Such impulsive behavior, which is actually the result of constructive interference of horizontally polarized waves, is most prominent in the fault-normal component of ground motion [1]. These pulses, which characterize FD ground motions, have an appreciable effect on spectral pseudo-acceleration (S_a) at periods around the pulse duration (or pulse period, T_p) [2].

Recently, advances have been made allowing such NS effects to be consistently included in probabilistic seismic hazard analysis (PSHA) [3,4], which refers to elastic structural demand. Moreover, inelastic structural response to pulse-like ground motions may be systematically different from that to non-impulsive, or *ordinary*, records, exhibiting heightened displacements at structural periods around one-half to one-third of T_p [5].

In this study, a discussion of the application of recent results about pulse-like seismic demand to non-linear static structural analysis procedures is addressed. The following is structured so that an introductory presentation of the displacement coefficient method (DCM) is first given. Then, evaluation of NS elastic (hazard) and inelastic seismic demand is described. Finally, the DCM in NS conditions is illustrated by means of an example and the outcome is discussed with respect to the ordinary case.

2 NON-LINEAR STATIC PROCEDURES

Estimating non-linear structural response is essential in the context of performance-based seismic design and assessment. Due to the relative inadequacy of elastic analysis on one hand, and the daunting complexity of non-linear dynamic analysis on the other, approximate procedures based on static non-linear analysis of structures were developed towards that end. Prominent among these are the DCM introduced in [6,7] and improved upon in [8] and the capacity spectrum method (CSM) [9].

The concept, which lies at the core of these methods, is that one first obtains a capacity (or “pushover”) force-displacement curve by loading a non-linear model of the structure with a predetermined profile of lateral forces which are gradually increased up to a point of collapse. This curve is subsequently used as the starting point to approximate the structure as a (typically bilinear) yielding single degree of freedom (SDoF) oscillator, whose spectral inelastic response (given the elastic demand) is used to estimate that of the original structure.

Inelastic response spectra required in the procedure mentioned above are traditionally derived from the statistical treatment of the responses of yielding SDoF oscillators subjected to a suite of recorded ground motions. These are usually presented in the form of strength reduction factor - ductility - period (R- μ -T) relations (e.g., [10]), or inelastic displacement ratio spectra (e.g., [11]) applicable in the DCM, as elaborated in the following sections.

3 DISPLACEMENT COEFFICIENT METHOD

3.1 Method description

The DCM attempts to estimate the inelastic displacement demand of the structure, which corresponds to a degree of freedom of reference and is termed the target displacement, δ_t , by

applying a succession of modification factors upon the elastic spectral response of an *equivalent* SDoF system, Equation (1):

$$\delta_t = C_0 \cdot C_1 \cdot C_2 \cdot C_3 \cdot S_a \cdot \frac{T^2}{4\pi^2} \quad (1)$$

S_a is the intensity measure chosen to represent elastic demand and forms the basis for design. It is derived from seismic hazard corresponding to the performance level considered; i.e., from design spectra. Thus $S_a \cdot (T^2/4\pi^2)$ represents elastic spectral displacement of the equivalent SDoF system having elastic period equal to T . Coefficients C_i $\{i = 0, 1, 2, 3\}$ are intended to transform this elastic response to inelastic structural response in a modular manner.

C_0 converts the displacement of the equivalent SDoF system into that of the original multiple degree of freedom (MDoF) structure and is given by Equation (2), where $[M]$ is the lumped mass matrix of the structure, $\{r\}$ is a vector coupling foundation motion with degrees of freedom of the structure, and vector $\{\phi\}$ is the generalized displacement used for the SDoF approximation, normalized so that unit value corresponds to the degree of freedom the target displacement refers to (e.g., the roof displacement). C_0 is the modal participation factor when $\{\phi\}$ is an eigenvector of the system.

$$C_0 = \frac{\{\phi\}^T [M] \{r\}}{\{\phi\}^T [M] \{\phi\}} \quad (2)$$

C_1 is termed the inelastic displacement ratio and is defined as the peak displacement response $S_{d,inel}$ of an inelastic SDoF system divided by the displacement of an indefinitely elastic SDoF oscillator with the same initial period, Equation (3).

$$C_1 = \frac{S_{d,inel}}{S_a \cdot (T^2/4\pi^2)} \quad (3)$$

In [8] it was recommended that C_1 be estimated from Equation (4), where the inelastic displacement ratio is given as a function of the period of vibration, strength reduction factor R and a site subsoil-dependent parameter α .

$$C_1 = 1 + \frac{(R-1)}{\alpha \cdot T^2} \quad (4)$$

The R factor appearing in Equation (4) is the reciprocal of structural yield strength normalized with respect to ground motion intensity and is given by Equation (5), where W is the weight of the structure, V_y is the base shear causing conventional yielding of the structure (to follow) and g is the acceleration of gravity. C_m is the percentage of total mass activated when the structure vibrates according to the displacement vector $\{\phi\}$.

$$R = \frac{S_a/g}{V_y/W} \cdot C_m = \frac{S_a/g}{V_y/W} \cdot C_0 \cdot \frac{\{\phi\}^T [M] \{r\}}{\{r\}^T [M] \{r\}} \quad (5)$$

C_2 is intended to account for the effect stiffness and/or strength degrading hysteretic behavior can have on maximum inelastic displacement.

Lastly, coefficient C_3 is intended to account for increased inelastic displacements in cases where second order (or P- Δ) effects become an important factor.

3.2 Inelastic displacement ratio of near-source pulse-like ground motions

In [12,13] and elsewhere, it was discussed that C_1 from Equation (4) is not explicitly representative of inelastic displacement ratios in the case of pulse-like ground motions in NS conditions. In [5], Equation (6) was proposed for the (constant-strength) inelastic displacement ratio C_R , based on a dataset of pulse-like FD ground motions identified as such in previous works [2,12]. Ordinary least squares estimators obtained for the parameters θ_i $\{i = 1, 2, 3, 4, 5\}$ appearing in Equation (6) are reported in [5].

$$C_R = \frac{S_{d,inel}}{S_a \cdot (T^2/4\pi^2)} = 1 + \theta_1 \cdot (T_p/T)^2 \cdot (R-1) + \theta_2 \cdot (T_p/T) \cdot \exp\left\{\theta_3 \cdot \left[\ln(T/T_p - 0.08)\right]^2\right\} + \theta_4 \cdot (T_p/T) \cdot \exp\left\{\theta_5 \cdot \left[\ln(T/T_p + 0.5 + 0.02 \cdot R)\right]^2\right\} \quad (6)$$

A graphical representation of Equation (6) is provided in Figure 1. The most important feature of this analytical model for C_R , is the use of normalized period T/T_p as a predictor variable in order to capture the spectral regions of amplification of inelastic response.

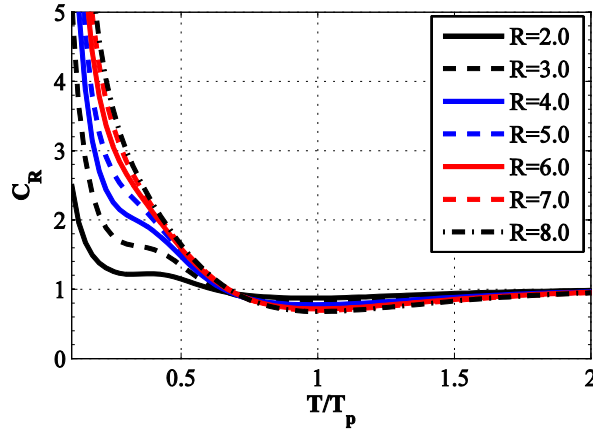


Figure 1: Model for the inelastic displacement ratio C_R of near-source pulse-like ground motions [5].

3.3 Other coefficients of displacement modification in NS conditions

The effect of cyclic structural degradation on peak inelastic displacement was investigated at the SDoF level in [13]. This effect would correspond to C_2 in the DCM. It was found that there is palpable increase in inelastic displacement for values of T/T_p less than 0.5, especially for cases of severe strength and stiffness degradation.* The present study deals with a code-conforming structure in the illustrative example given below, and the C_2 coefficient is constrained to unity in what follows.

In [14] it is reported that pulse-like ground motions may be more sensitive to phenomena of dynamic instability due to P- Δ effects than non-pulse-like ground motions. However, this issue being outside the scopes of the study, the C_3 coefficient is also taken as unity herein.

* In [13] it is also reported that such effects as there are, they tend to wane with increasing strength reduction factors. This is in contrast with the trend of the equation suggested in [8].

4 NEAR-SOURCE SEISMIC HAZARD AND INELASTIC DEMAND

4.1 Near-source probabilistic seismic hazard analysis

Near-source probabilistic seismic hazard analysis (NS-PSHA [3,4]) at present state computes the mean annual frequency (λ) of exceedance of an intensity measure value, spectral acceleration hereafter, as a linear combination of two hazard terms, one accounting for absence of pulse ($\lambda_{S_a, \text{no pulse}}$) and one for pulse occurrence ($\lambda_{S_a, \text{pulse}}$) as shown in Equation (7).

$$\lambda_{S_a}(s_a) = \lambda_{S_a, \text{no pulse}}(s_a) + \lambda_{S_a, \text{pulse}}(s_a) \quad (7)$$

In the NS case, the first term on the right-hand side of Equation (7) is calculated by implementing some modifications to classical PSHA [15] resulting in the integral shown in Equation (8a) for a single fault scenario. The contribution of pulse-like ground motions to hazard is expressed by the second right-hand term of Equation (7) which is given in Equation (8b).

$$\lambda_{S_a, \text{no pulse}}(s_a) = v \cdot \int \int_{m, \underline{z}} P[\text{nopulse} | m, \underline{z}] \cdot G_{S_a | M, \underline{z}}(s_a | m, \underline{z}) \cdot f_{M, \underline{z}}(m, \underline{z}) \cdot dm \cdot d\underline{z} \quad (8a)$$

$$\lambda_{S_a, \text{pulse}}(s_a) = v \cdot \int \int \int_{m, \underline{z}, t_p} P[\text{pulse} | m, \underline{z}] \cdot G_{S_a, \text{mod} | M, \underline{z}, T_p}(s_a | m, \underline{z}, t_p) \cdot f_{T_p | M, \underline{z}}(t_p | m, \underline{z}) \cdot f_{M, \underline{z}}(m, \underline{z}) \cdot dm \cdot d\underline{z} \cdot dt_p \quad (8b)$$

In these equations v is the annual rate of event occurrence on the source, and M is the moment magnitude (not to be confused with the mass matrix appearing in Section 3). A relationship between M and rupture dimensions is used in order to derive the joint probability density function, or PDF, $f_{M, \underline{z}}$ [16]. In this case, source-site distance is only one of the variables included in the vector of rupture-site geometry parameters, \underline{z} , which is required in order to evaluate the probability of pulse occurrence, $P[\text{pulse} | m, \underline{z}]$ [17]. Additionally, G_{S_a} indicates a complementary cumulative distribution function (CCDF) defined by an ordinary ground motion prediction equation (GMPE), while $G_{S_a, \text{mod}}$ represents a GMPE suitably modified to account for NS-FD spectral shape [2][†]. The PDF $f_{T_p | M, \underline{z}}$ is taken from an empirical model of T_p [12]. More details on NS-PSHA are in [4].

4.2 Hazard disaggregation and near-source inelastic demand

Once NS-PSHA calculations are completed, disaggregation of seismic hazard can be carried out for any s_a . This procedure provides the probability distribution of the covariates appearing in Equations (8a,b) conditional, for example, on exceedance of s_a [4]. In this case, the distribution of pulse period $f_{T_p | S_a(T) > s_a}$ (implicitly also conditional on pulse occurrence) is relevant in the implementation of the DCM in NS conditions, since pulse period T_p enters Equation (6) determining expected inelastic demand.

However, NS hazard includes contributions from pulse-like ground motions with infinite in number possible pulse periods. Therefore, one needs the probability density $f_{T_p | S_a(T) > s_a}$ in order to marginalize the expectation function of C_R according to Equation (9).

[†] In a recent paper [18], a modified GMPE was proposed for the non-impulsive case as well.

$$E[C_R | S_a(T) > s_a] = \int_{t_p} E[C_R | S_a(T) > s_a, T_p = x] \cdot f_{T_p|S_a(T) > s_a}(x) \cdot dx \quad (9)$$

Apart from the marginal PDFs of pulse period, one more useful result can be obtained from disaggregation of NS hazard, namely, the conditional probability of pulse occurrence given that $S_a > s_a$. This may be used to also estimate the NS inelastic demand $\delta_{t,NS}$, via the conditional expectation theorem, as an average of two separate contributions, target displacements given pulse occurrence $\delta_{t,pulse}$ and absence thereof $\delta_{t,no pulse}$. These two terms are weighted by their probability of occurrence conditional to the scenario of interest, Equation (10).

$$\delta_{t,NS} = \delta_{t,pulse} \cdot P[\text{pulse} | S_a > s_a] + \delta_{t,no pulse} \cdot (1 - P[\text{pulse} | S_a > s_a]) \quad (10)$$

A simpler alternative could be to assume the target displacement equal to the largest estimate between impulsive and non-impulsive inelastic demand. Note, however, that this may be conservative since, even in sites particularly prone to directivity effects, marginal pulse occurrence probability is hardly close to one [17].

5 ILLUSTRATIVE APPLICATION

5.1 Design scenario in NS conditions

For the purpose of the present study, a NS design scenario was considered, where the site to source configuration is prone to FD effects – intentionally so. This is illustrated in Figure 2(a), which shows a plan view of a 200 km long strike-slip fault and a site of interest perfectly aligned with the fault at a distance of 5 km off the tip.

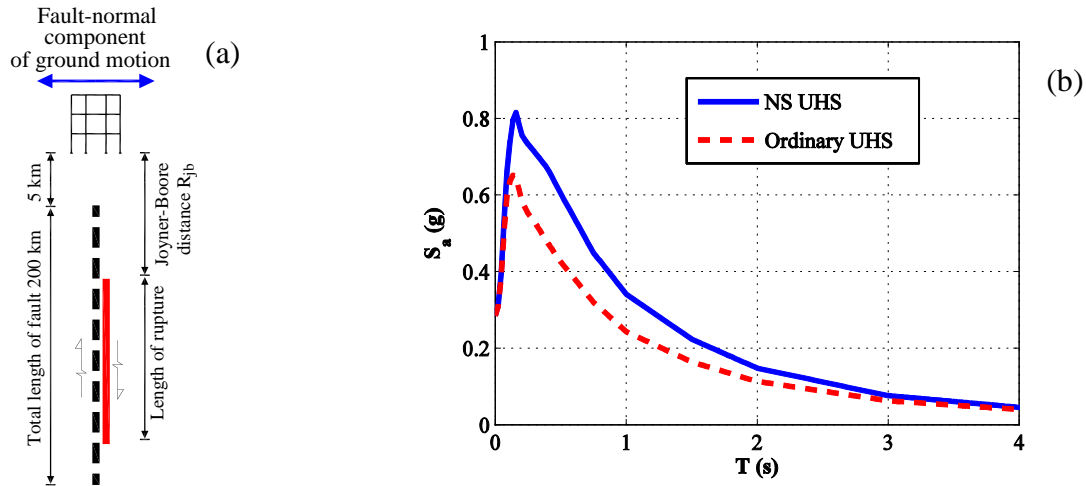


Figure 2: Schematic representation of design scenario (a) and UHS for a 2475 yr return period resulting from NS and ordinary PSHA (b).

Subsoil conditions at the site were taken to correspond to stiff soil deposits and an annual rate of event recurrence on the fault $\nu = 0.20$ was arbitrarily assumed, along with unit negative slope for the Gutenberg-Richter [19] relationship defined between M 4.5 and M 7.5. Seismic hazard was calculated through modified NS-PSHA (from Section 4) resulting in the 2475 yr uniform hazard spectrum (UHS) in Figure 2(b); in the figure the UHS derived by ordinary PSHA is also reported.

Given that in the following section a structure with a first-mode natural period of vibration $T = 0.75\text{s}$ is considered, disaggregation of NS hazard was sought conditional on exceedance of s_a from the 2475 yr UHS at this period. The PDF of T_p thus obtained is shown in Figure 3.

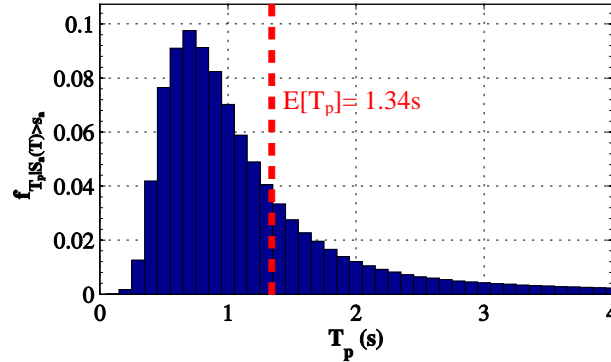


Figure 3: Probability density function resulting from NS hazard disaggregation conditional on pulse occurrence and $S_a(T) > s_a$, referring to 2745yr return period at the site, for $T = 0.75\text{s}$ (histogram normalized to unit area).

5.2 Implementation of the displacement coefficient method in near-source conditions

For an illustrative application of the DCM in NS conditions, a specific structure was considered at the fictitious site described in the above section. The structure in question is a 5-storey bare (non-infilled) reinforced concrete (R/C) frame corresponding to the internal frames of a perfectly symmetric building (Figure 4). This frame was chosen to correspond to a first-mode period of natural vibration $T_1 = 0.75\text{s}$ (in the direction normal to the fault's strike, Figure 2). Furthermore, structure geometry was selected so that this plane frame would exhibit first-mode dominated dynamic elastic response (first mode participation ratios in excess of 80%) and flexure-dominated inelastic response.

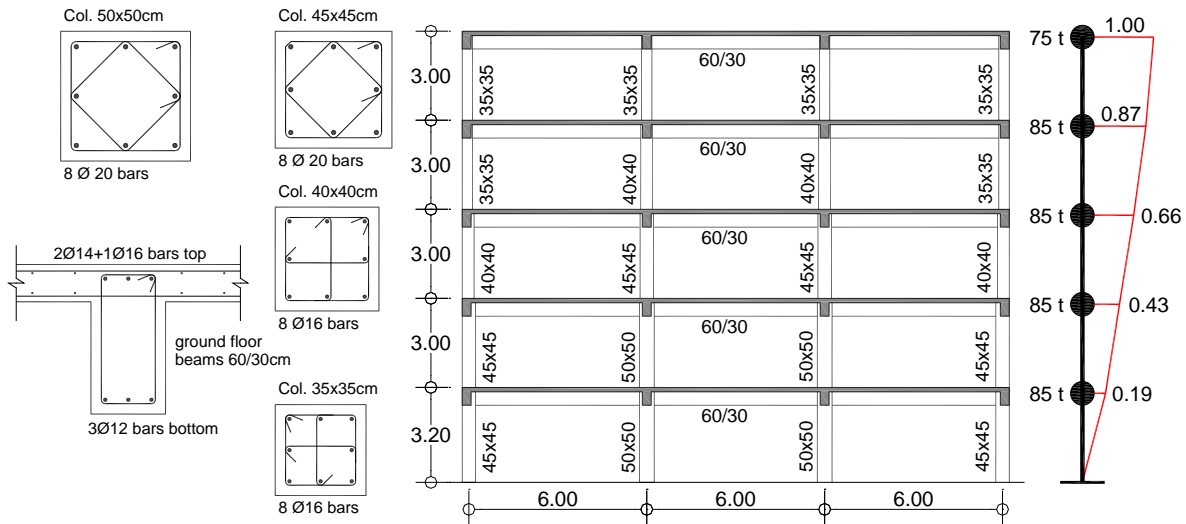


Figure 4: Summary of design details and MDoF model characteristics for a 5-storey plane R/C frame used in this study corresponding to a first mode period of vibration $T = 0.75\text{s}$.

The structure was designed according to modern codes [20,21] against gravity loads and seismic actions. The design spectrum was considered to be a site-specific UHS obtained by classical PSHA. More specifically, the frame was designed for inelastic response corresponding to a *behavior factor* ≈ 3.0 under the actions of a 475 yr return period (T_R) ordinary UHS.

Material qualities assumed for design were C20/25 for concrete and S500/550 for reinforcing steel [20]. A sample of the resulting detailing can also be seen in Figure 4.

Given that a modern-code-designed structure possessing significant reserves of over-strength is unlikely to exhibit inelastic response corresponding to a large strength reduction factor for a *life safety* performance level ($T_R = 475$ yr), the following example focuses on a *collapse prevention* performance level ($T_R = 2475$ yr).

First, a pushover (base shear – roof displacement) curve was obtained for the structure (shown in Figure 5 as gray dashed line). The non-linear structural model built for this inelastic static analysis, used lumped plasticity multi-linear moment-rotation envelopes and a smeared crack approach for modeling elastic stiffness of R/C members. Moment-rotation relationships for each member were estimated using mean strength and stiffness properties for confined concrete [22] and reinforcing steel. The bilinear approximations of the resulting relations used the *collapse prevention* limiting values recommended in [7] for ultimate rotation capacity.

The non-linear static analysis was carried out by applying a gradually increasing lateral deformation profile which remained unchanged throughout the analysis and corresponds to the structure's first mode eigenvector (shown in Figure 4).

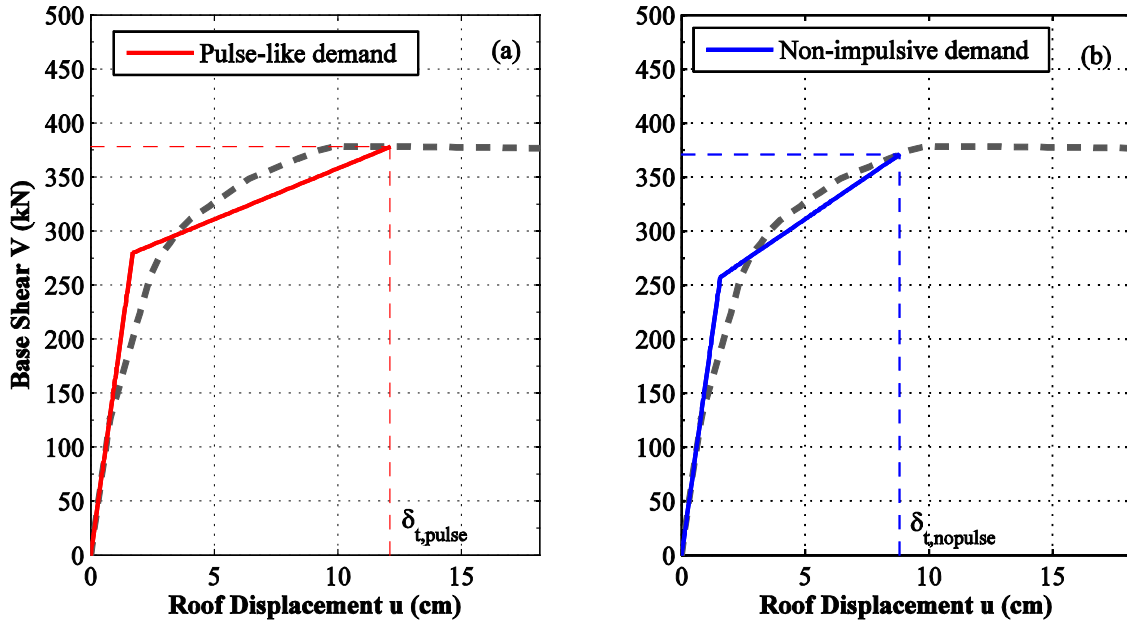


Figure 5: Graphical representation of application of the DCM static non-linear procedure for the 5-storey R/C frame considered. Target displacement estimates for the collapse prevention performance level considering impulsive (a) and non-impulsive contributions (b).

In estimating the right-hand-side of Equation (10), the non-impulsive contribution $\delta_{t,no\ pulse}$ was obtained by simple implementation of the DCM using Equation (4) for coefficient C_1 , taking subsoil coefficient α to correspond to NEHRP class C [8]. The same process was repeated for the impulsive contribution $\delta_{t,pulse}$, with the difference that Equation (6) and Equation (9) have to be used to substitute coefficient C_1 with the inelastic displacement ratio C_R for FD ground motions.

In order to calculate these target displacements using the DCM, a bilinear approximation of the capacity (pushover) curve was constructed according to the methodology suggested in [7]. This method requires the bilinear approximation to intersect the pushover curve at δ_t thus resulting in some (usually) positive post-yield stiffness or hardening. This hardening behavior is

typically ignored when estimating C_1 via Equation (4); however, this matter will not be discussed here. Additionally, this bilinearization method implies that the point corresponding to conventional yield base shear V_y is dependent on target displacement δ_t , thus requiring some iterations before convergence to an R and corresponding δ_t value. A graphical representation (corresponding to the converged iteration) for each of the two contributions considered in Equation (10), is provided in Figure 5. Both operations described above use the NS UHS of Figure 2 to calculate elastic demand.

For reasons of comparison, an ordinary target displacement $\delta_{t,ord}$ was also evaluated using the classical DCM and the non-impulsive UHS (red dashed line in Figure 2b) for elastic demand. It is worth noting that $\delta_{t,no\ pulse}$ and $\delta_{t,ord}$ are both derived by following the same procedure applied to different estimates of elastic demand (NS and ordinary UHS respectively), which means that $\delta_{t,no\ pulse}$ would be the target displacement if NS conditions were only accounted for during hazard calculations.

To obtain the final estimate of target displacement $\delta_{t,NS}$ for the considered site, one also requires the pulse occurrence probability conditional to the hazard threshold, which is equal to 0.747. Thus from Equation (10), $\delta_{t,NS}$ is found to be equal to 113 mm, which is 85% more than $\delta_{t,ord}$. All numerical results are summarized in Table 1.

$\delta_{t,pulse}$ (mm)	$\delta_{t,no\ pulse}$ (mm)	$P[\text{pulse} S_a > s_a]$	$\delta_{t,NS}$ (mm)	$\delta_{t,ord}$ (mm)	$\frac{\delta_{t,NS} - \delta_{t,ord}}{\delta_{t,ord}}$
121	88	0.747	113	61	85%

Table 1: Summary of target displacement estimate resulting from DCM application. All values refer to collapse prevention limit state (i.e. $T_R = 2475\text{yr}$).

Instead of using entire probability densities obtained from disaggregation of seismic hazard, as in Equation (9), a first moment approximation may be obtained by using the average pulse period, $E[T_P]$, from Figure 3 as per Equation (11).

$$E[C_R | S_a(T) > s_a] \approx E[C_R | S_a(T) > s_a, T_P = E[T_P]] \quad (11)$$

In the present example, Equation (9) resulted in $E[C_R] = 1.47$ while the approximation of Equation (11) would give $E[C_R] \approx 1.33$, resulting in an estimated inelastic displacement, due to impulsive ground motions, of 109 mm – compare that with 121 mm in Table 1.

6 CONCLUSIONS

The study dealt with implementing static non-linear procedures in order to estimate inelastic structural demand in near-source conditions. First, a brief overview of the original procedure for estimating target displacement using the DCM was given. Subsequently, the modifications required in order to account for NS conditions were discussed, both in terms of elastic (i.e., seismic hazard) and inelastic displacement demand. Then, a procedure for the implementation of the DCM in a NS context was outlined, considering a single-fault NS design scenario and finally, an illustrative example was provided.

The structure considered in the example was a code-conforming R/C frame designed against seismic demand corresponding to ordinary site-specific hazard. The site was intentionally assumed to have a disadvantageous location with respect to expected directivity ef-

fects. After computing UHS from ordinary- and NS-PSHA, a non-linear static analysis of the frame was carried out and the capacity curve obtained was used to derive a bilinear SDoF approximation of the structure. Furthermore, NS hazard disaggregation was calculated conditional on $S_a(T) > s_a$ at the period corresponding to the SDoF approximation and for a return period of 2475 yr. The resulting PDF of pulse period was combined with a predictive model for inelastic SDoF response to pulse-like ground motions in order to estimate NS displacement demand.

It was shown that, in the case examined, NS inelastic structural demand can considerably exceed demand as computed without accounting for FD in non-linear static analysis procedures.

ACKNOWLEDGMENTS

The study presented in this paper was developed within the activities of Rete dei Laboratori Universitari di Ingegneria Sismica (ReLUIS) for the research program funded by the Dipartimento della Protezione Civile (2010-2013).

REFERENCES

- [1] P.G. Somerville, N.F. Smith, R.W. Graves, N.A. Abrahamson, Modification of empirical strong ground motion attenuation relations to include the amplitude and duration effects of rupture directivity. *Seismological Research Letters*, **68**, 199-222, 1997.
- [2] J.W. Baker, Identification of near-fault velocity and prediction of resulting response spectra. *Proceedings of Geotechnical Earthquake Engineering and Structural Dynamics IV*, Sacramento, CA, 2008.
- [3] P. Tothong, C.A. Cornell, J.W. Baker, Explicit directivity-pulse inclusion in probabilistic seismic hazard analysis. *Earthquake Spectra*, **23**, 867-891, 2007.
- [4] E. Chioccarelli, I. Iervolino, Near-source seismic hazard and design scenarios. *Earthquake Engineering & Structural Dynamics*, **42**, 603-622, 2013.
- [5] I. Iervolino, E. Chioccarelli, G. Baltzopoulos, Inelastic Displacement Ratio of Near-Source Pulse-like Ground Motions. *Earthquake Engineering & Structural Dynamics*, **41**, 2351-2357, 2012.
- [6] BSSC, *NEHRP guidelines for the seismic rehabilitation of buildings*, FEMA-273, developed by ATC for FEMA, Washington, D.C., 1997.
- [7] ASCE, *Prestandard and Commentary for the Seismic Rehabilitation of Buildings*, FEMA-356, developed by ASCE for FEMA, Washington, D.C., 2000.
- [8] FEMA, Improvement of nonlinear static seismic analysis procedures, FEMA-440 prepared by ATC, Washington, D.C., 2005.
- [9] P. Fajfar, Capacity Spectrum Method Based on Inelastic Demand Spectra. *Earthquake Engineering and Structural Dynamics*, **28**, 979-993, 1999.
- [10] T. Vidic, P. Fajfar, M. Fischinger, Consistent Inelastic Design Spectra: Strength and Displacement. *Earthquake Engineering & Structural Dynamics*, **23**, 507-521, 1994.
- [11] J. Ruiz-García, E. Miranda, Inelastic displacement ratios for evaluation of existing Structures. *Earthquake Engineering and Structural Dynamics*, **32**(9), 1237-1258, 2003.

- [12] E. Chioccarelli, I. Iervolino, Near-source seismic demand and pulse-like records: A discussion for L'Aquila earthquake. *Earthquake Engineering and Structural Dynamics*, **39**, 1039-1062, 2010.
- [13] J. Ruiz-García, Inelastic Displacement Ratios for Seismic Assessment of Structures Subjected to Forward-Directivity Near-Fault Ground Motions. *Journal of Earthquake Engineering*, **15**(3), 449-468, 2011.
- [14] B. Alavi, H. Krawinkler, Behavior of moment-resisting frame structures subjected to near-fault ground motions. *Earthquake Engineering and Structural Dynamics*, **33**(6), 687-706, 2004.
- [15] L. Reiter, *Earthquake hazard analysis, issues and insights*. NY: Columbia University Press, 1990.
- [16] D.L. Wells, K.J. Coppersmith, New empirical relationships among magnitude, rupture length, rupture width, rupture area, and surface displacement. *Bulletin of the Seismological Society of America*, **87**(4), 974-1002, 1994.
- [17] I. Iervolino, C.A. Cornell, Probability of occurrence of velocity pulses in near-source ground motions. *Bulletin of the Seismological Society of America*, **98**(5), 2262-2277, 2008.
- [18] S. Shahi, and J.W. Baker, An empirically calibrated framework for including the effects of near-fault directivity in probabilistic seismic hazard analysis. *Bulletin of the Seismological Society of America*, **101**(2), 742-755, 2011.
- [19] B. Gutenberg, C.F. Richter, Frequency of Earthquakes in California. *Bulletin of the Seismological Society of America*; **34**, 185-188, 1944.
- [20] CEN, *EN 1992-1-1 Design of concrete structures. General rules and rules for buildings*, European Committee for Standardization, Brussels, 2004.
- [21] CEN, *EN 1998-1 Design of structures for earthquake resistance – Part 1: General rules seismic actions and rules for buildings*, European Committee for Standardization, Brussels, 2004.
- [22] J.B. Mander, M.J.N. Priestley, R. Park, Theoretical Stress-Strain Model for Confined Concrete. *Journal of Structural Engineering*, **114**(8), 1804-1826, 1988.